The Journal of Undergraduate Research

Volume 9 *Journal of Undergraduate Research, Volume 9: 2011*

Article 15

2011

Vibrational Analysis of Soloflex Whole Body Vibration Platform

Zachary Croatt
South Dakota State University

Josh Robers
South Dakota State University

Vibrational Analysis of Soloflex Whole Body Vibration Platform

Authors: Zachary Croatt,* Josh Robers†
Faculty Sponsors: Dr. Shawn Duan,* Dr. Teresa Binkley†
Departments: *Mechanical Engineering,
†Ethel Austin Martin Program in Human Nutrition

ABSTRACT

A Soloflex Whole Body Vibration (WBV) Platform was tested for its frequency and magnitude of vibration at multiple settings on the supplied dial. An accelerometer was used to measure the vibrations on different points mapped across the platform. The motor attached to the board was also tested for its frequency using a high-speed camera. The amplitude measurements found from the accelerometer data was compared to the readings on the supplied control module to "calibrate" the platform for medical testing.

Keywords: vibration, whole body vibration plate, bone density

INTRODUCTION

Whole body vibration platforms have become increasingly popular for home use as well as use in gyms for professional athletes. The company leading the market in this area is

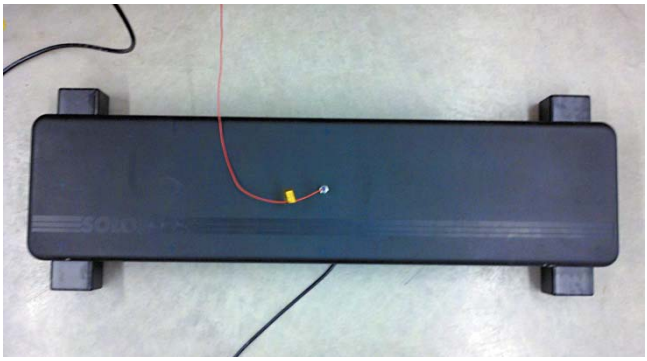

Soloflex. Figure 1 below shows the platform that was used for the testing and research.
Figure 1. Soloflex Whole Body Vibration Platform

The platform for this project was analyzed for medical research. The platform is going to be used to test the theory that children's bones stimulated with vibration will gain more

density than children without the same treatment. The plate needs to be analyzed to ensure that the testing is controlled. The testing data was compared to settings printed on the control module supplied with the platform. This was done to ensure the medical researchers know exactly what amplitude and frequency of vibration their test subjects will receive. The tested board will also be used for calibration of other boards used with different test subjects.

METHODS

Materials

The test setup can be seen in the figures below and table 1 shows the equipment and its information. Figure 1 shows the oscilloscope and the signal conditioner used to record the data from the accelerometer. The platform was attached to a heavy table to ensure the board did not move and would not excite what it was resting on. This is shown in figure 2. Finally the control module that was supplied with the board is shown in figure 4.

Equipment			
Type	Brand	Model #	Serial #
Four Channel Digital Storage Oscilloscope	Tektronics	TDS 2024B	C033112
Signal Conditioner	Endevco	133	CB71
Accelerometer	Columbia	5005 HT	1521
Soloflex WBV Platform	Soloflex		

Table 1. Equipment [1-3]

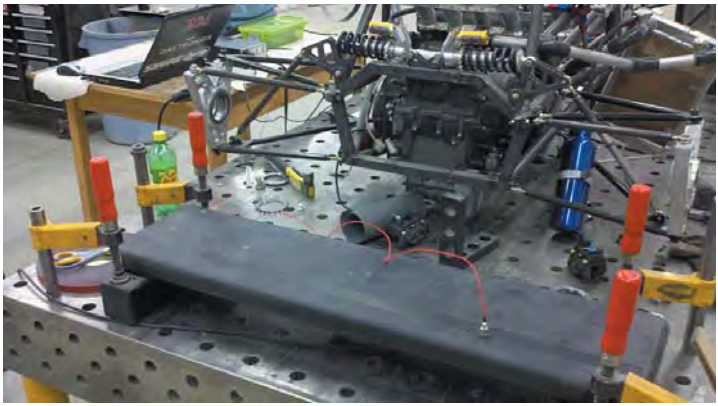

Figure 2. Signal Conditioner and Oscilloscope

Figure 3. WBV Platform Clamped to a Large Fixture Table
Figure 4. Supplied Control Module

Methods

The first assumption to simplify and accelerate the test was to consider the vibration of the platform to be symmetrical. Points were then marked on the platform as shown in figure 5 below. The accelerometer was placed at each point and a time history of the vibration was recorded, using the oscilloscope and a signal conditioner, at 3 different settings on the supplied control module: 0.3 g, 0.7 g and 1.0 g. The data taken for each point and each setting was graphed and analyzed to find the magnitude and frequency of the vibration at each point on the board. Because the user would not have their legs spread as far as the grid was made, only points D – L were used in testing.

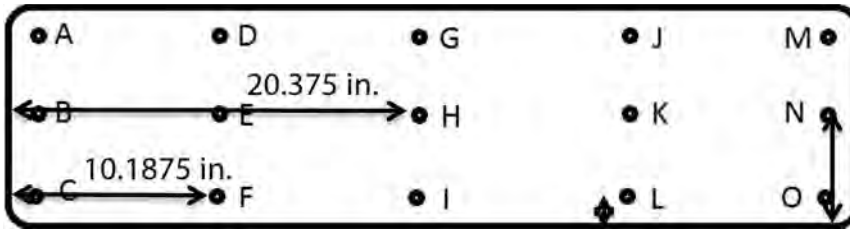

Figure 5. Test Point Map

RESULTS

The recorded data were compared to the data shown in the FAQ section of the Soloflex website, which is shown below [4]:

.3 g's = 28 Hz
.5 g's = 30 Hz
.7 g's = 35 Hz
.8 g's = 45 Hz
.9 g's = 50 Hz
1.0 g = 55 Hz
1.1 g's = 60 Hz

The data in the tables below shows the recorded data for points E and H of figure 5. These data were compared to the data from the Soloflex website as well as between the two pints themselves.

Dial Setting (g)	Accelerometer Reading (g)	Acceleration % Difference	Accelerometer Frequency (Hz)	Soloflex Frequency (Hz)	Frequency % Difference
0.3	0.16	46.67	40.11	28	43.25
0.5	0.234	53.2	46.59	30	55.3
0.7	0.364	48	46.82	35	33.77
0.8	0.59	26.25	48.79	45	8.42
0.9	0.74	17.78	49.12	50	1.76
1	0.96	4	49.89	55	9.29
1.1	1.01	8.18	50.28	60	16.2

Table 2. Point E Data

Table 3. Point H Data

Dial Setting (g)	Accelerometer Reading (g)	Acceleration % Difference	Accelerometer Frequency (Hz)	Soloflex Frequency (Hz)	Frequency % Difference
0.3	0.16	46.67	40.26	28	43.79
0.5	0.336	32.8	44.37	30	47.9
0.7	0.612	12.57	46.48	35	32.8
0.8	0.92	15	47.54	45	5.64
0.9	1.36	51.11	49.02	50	1.96
1	1.67	67	49.29	55	10.38
1.1	1.75	59.09	49.63	60	17.28

Table 4. Comparison of Point E and Point H Data

Dial Setting (g)	Middle Acceleration (g)	Left-Middle Acceleration (g)	Percent Difference
0.3	0.16	0.16	0
0.5	0.336	0.234	30.36
0.7	0.612	0.364	40.52
0.8	0.92	0.59	35.87
0.9	1.36	0.74	45.59
1	1.67	0.96	42.51
1.1	1.75	1.01	42.29

The following two figures are examples of the recorded curves from each test point.

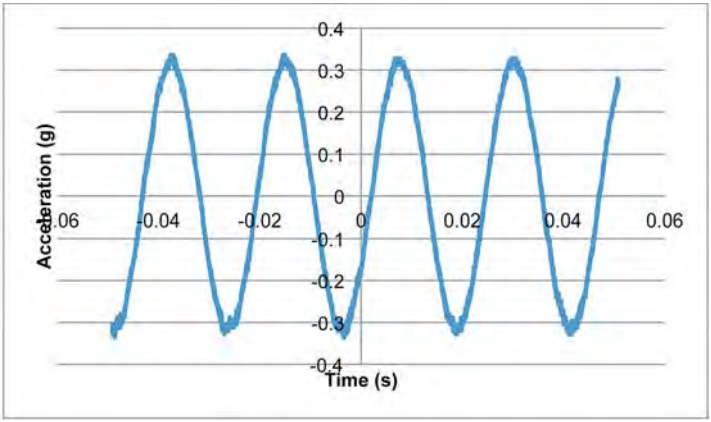

Figure 6. Point H 0.5 g Dial Setting

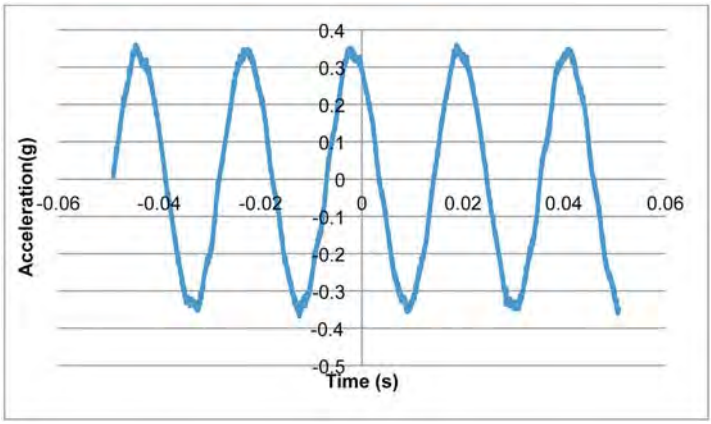

Figure 7. Point E 0.5g Dial Setting

DISCUSSION

It can be seen in the tables above that the dial settings are inaccurate when compared to the accelerometer data that was recorded. The data for point E was consistently lower than the reading the dial was set to. The point H data was lower until the 0.8 g dial setting and then it became greater. Some dial settings for both points had low differences while some had very great differences.

Comparing the point accelerations to each other shows some great differences but this was to be expected because of factors such as, distance from the motor and distance from the supports.

The frequency readings were calculated from the average period of the recorded vibration wave. These frequency readings, when compared to the Soloflex website data, had very large differences except for the 0.9 g dial setting. The point frequencies, however, were very similar.

LIMITATIONS

The vibration of the plate would be greatly affected if the same test had been conducted with a mass on the platform.

REFERENCES

[1] Endevco, User Manual for Endevco 133 Signal Conditioner
[2] Columbia Research Lab, Calibration data form for 5005 HT Accelerometer
[3] Tektronics, Inc. User Manual for TDS 2024B Oscilloscope
[4] Soloflex, Inc. FAQs, 2009, http://www.soloflex.com/whole-body-vibration/faqs/

Biosolar Conversion of N_2 and H_2O to Ammonia by Engineered N_2-fixing Cyanobacteria

Author: Seth T. Harris
Faculty Sponsor: Ruanbao Zhou
Department: Biology & Microbiology

ABSTRACT

The cyanobacterium *Anabaena* sp. PCC 7120 is capable of using solar energy to produce ammonia through conversion of atmospheric dinitrogen in differentiated cells called heterocysts. Harnessing this system could enable cyanobacteria to be used in ammonia-fertilizer production, creating a renewable alternative to the current Haber-Bosch process. The genes *patA* and *alr3304* in the *Anabaena* 7120 genome are important in heterocyst formation; an increase in heterocyst formation is seen with over-expression of *patA* or inactivation of *alr3304*. This research aims to create a novel mutant that forms more heterocysts by simultaneously over-expressing *patA* and inactivating *alr3304*, producing higher amounts of ammonia. These two genes were isolated using Polymerase Chain Reaction (PCR) amplification. The resulting amplicons were then inserted into pTOPO 2.1 vectors, creating pZR855 and pZR854, respectively. *PatA* was removed from pZR855 using enzymatic digestion and then ligated into pZR618 to create pZR856, which enabled the successful transformation of NEB 10-beta *Escherichia coli* competent cells with pZR856 and later plasmids. Plasmid pZR857 was created by fusing *patA* from pZR856 to the native *Anabaena* promoter *PpsbA* in pZR811. The 2.7kb fragment *PpsbA-patA* was inserted within *alr3304* in pZR854 to create pZR858, thereby disrupting *alr3304*. PCR and sequencing were used to verify different stages of the plasmid constructions. Results from colony PCR and enzymatic digestion indicated that pZR858 was successfully created. Further progression in this research will potentially create a mutant strain of *Anabaena* 7120 that forms more heterocysts and therefore produces ammonia at a commercially viable level.

INTRODUCTION

The current process for converting atmospheric nitrogen to ammonia is through a synthetic process known as the Haber-Bosch process. This method utilizes various fossil fuels for energy and involves high temperatures and pressures to create the desired ammonia, which means large energy inputs. In fact, the Haber-Bosch process accounts for more than 1% of the total energy that is used by humans (9). When this energy requirement is broken down to just the fertilizer production market, specifically ammonia production, astonishing results are seen. The energy required to produce ammonia, the main ingredient in almost all nitrogen

fertilizers, is 87% of the energy consumed by the industry (4). To help alleviate the cost of fossil fuel consumption, the Haber-Bosch process has adapted many types of fossil fuels. Oil, coal, and even natural gas are now used in the process of creating ammonia; however, with the rising price of oil and the decreasing availability of petroleum, the cost of energy for making synthetic ammonia will increase dramatically (3).

The enormous requirement of fossil fuels is not the only drawback of the Haber-Bosch process. Along with the energy consumption are the greenhouse gasses (GHGs) produced as byproducts of the ammonia production. These GHGs that are produced include carbon dioxide, methane and nitrous oxide; 98% of the mass emitted is carbon dioxide while 0.6% is N_2O (11). Both carbon dioxide and nitrous oxide are important factors in global warming. The overall industry produces about 465 Tg CO_2-eq (Equivalent Carbon Dioxide) through the process of fertilizer manufacturing (4). With the high cost of energy and the environmental impact caused by GHGs, the Haber-Bosch process will need to be retired for a renewable, efficient, and environmentally friendly alternative. A promising candidate is the usage of cyanobacteria, which create ammonia as a product of its metabolism within specially differentiated heterocysts.

Cyanobacteria are microorganisms that have evolved over billions of years, thus gaining the ability to use solar energy through photosynthesis. This unique organism, specifically *Anabaena* sp. strain PCC 7120, is a filamentous cyanobacterium and has developed a metabolic pathway to create ammonia from atmospheric dinitrogen in specialized cells named heterocysts. These specialized cells create a microoxic environment which allows the O_2-labile enzyme nitrogenase to convert the dinitrogen to ammonia (1). When environmental ammonia levels become depleted, approximately every tenth vegetative cell differentiates into a heterocyst in order to produce ammonia for surrounding vegetative cells. The necessary nitrogenase is tightly regulated and only made within heterocysts (2).

The regulation of heterocyst formation is still widely being researched, but numerous genes have been identified that play a role in the conversion from vegetative cell to heterocyst. A major controlling factor in the regulation of heterocyst formation, and an intricate part of this research, is *patA*. PatA is one of two necessary proteins for heterocyst formation, mutant Anabaena without *patA* showed significant decrease in the ability to form heterocysts (8). The role that PatA plays in the formation of heterocysts is still unanswered. However, Orozco et al. (7) proposes that PatA, HetN, and PatS all play an important role in heterocyst formation and that PatA interacts with both PatS and HetN signaling pathways in a way that overcomes the inhibitory effects of the two pathways on heterocyst formation, both the HetN and PatS pathways caused a decrease in heterocyst formation when *patA* was deleted.

Another gene that plays an important role in heterocyst formation is *alr3304*, which has the ability to prevent heterocyst formation at specific stages of development (10). However, research showed that the silencing of *alr3304* decreases the ratio of vegetative cells to heterocysts, 5.3 in the mutant compared to the wildtype ratio of around 9 (10). Such a result leads to the conclusion that Alr3304 has some inhibitory effect on heterocyst formation. On the contrary, the over-expression of *patA* increases the ratio of heterocysts to vegetative cells (5). Theoretically, the combination of these two mutants could produce a novel *Anabaena* mutant with a higher ratio of heterocysts to vegetative cells than either of the single mutations (desired mutant in Fig. 1).

Overall, by silencing *alr3304* with an insertion of *patA*, the combined over-expression of *patA* and knock-out of *alr3304* could potentially create a strain of *Anabaena* able to form more heterocysts and produce ammonia at a concentration that is commercially viable. Such a mutant could reduce the usage of fossil fuels from the production of ammonia and decrease the GHGs released into the atmosphere by replacing the Haber-Bosch process. This alternative method utilizing cyanobacteria would also be a renewable source of ammonia, powered by clean, cheap, and readily available solar energy.

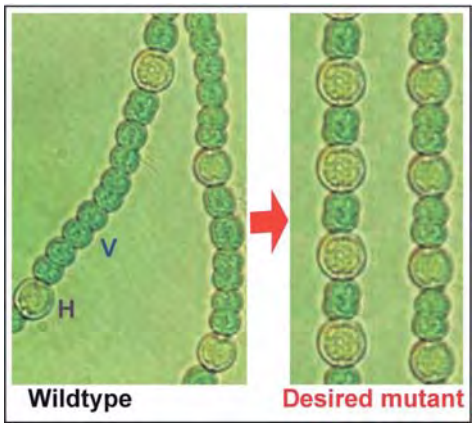

Figure 1. Projected *Anabaena* mutant. The cell indicated by H represents a heterocyst while the cell indicated by V is a vegetative cell. The desired *patA*$^+$/*alr3304*$^-$ *Anabaena* mutant is projected to have a higher ratio of heterocysts as compared to the wildtype and *patA*$^+$ or *alr3304*$^-$ mutants.

METHODS

Bacterial Strains and Growth Conditions

Top10 *Escherichia coli* competent cells were used with pTOPO 2.1 vectors for initial bacterial transformation. Subsequent bacterial transformations utilized NEB 10-beta *E. coli* competent cells. All *E. coli* were grown at 37˚C in a bacterial incubator. Luria Bertani (LB) agar was used for all growth media. Antibiotics were added to the LB agar for selection of transformed *E. coli* in appropriate concentrations. *Anabaena* sp. PCC 7120 was grown at 30˚C in flasks containing AA/8(N) liquid media under fluorescent lights or sunlight.

Gene Amplification

Chromosomal DNA from *Anabaena* 7120 was used in PCR to amplify the genes *patA* (1.2 kb) and *alr3304* (3.0 kb). Specific upstream and downstream primers (Table 1) created by our lab were used to amplify the target sequences. All PCR used the same program parameters of 94˚C to denature the DNA, followed by an annealing temperature of 50˚C,

and the standard Taq DNA Polymerase elongation temperature of 72˚C. Gel electrophoresis was used with 0.8% agarose gels containing ethidium bromide (EB). Gels were run at a constant 170mA submerged in 1xTAE using a gel box apparatus. Ultraviolet Violet light imaging of the gels after gel electrophoresis was done to visualize the DNA banding.

Table 1. PCR Primers. Primer sequences are listed from 5' to 3'.

Primer	Sequence	Notes
M13F	GTAAAACGACGGCCAG	Upstream primer for recombinant pTOPO
M13R	CAGGAAACAGCTATGAC	Downstream primer for recombinant pTOPO
T7	TTAATACGACTCACTATAGGG	Anneals to T7 promoter
T7 term	GGGTTATGCTAGTTATTGCTC	Anneals to T7 terminator
ZR127	CGTACCGGTGTCGACTCGCGCAATT-GCTAGCTTAAGACGTCAT	Anneal to ClaI region in pZR811
ZR191	TGGATCCTGAGGATTCACCTTTAGCC	Upstream for *alr3304*
ZR192	TCTCGAGTAGATTACGAAATTTCAGTAC	Downstream for *alr3304*
ZR193	TCATATGGGATCCATGAAAACACTTCCGATTAC	Upstream for *patA*
ZR194	TGTCGACCGTAATGTGTTTAAAAATTACT	Downstream for *patA*

Bacterial Transformation

PatA and *alr3304* were inserted into separate TOPO 2.1 *E. coli* vector plasmids, containing both kanamycin and ampicillin resistance. X-Gal was used to identify the colonies that received the inserted genes; white colonies had a disruption in the beta-galactosidase (*lacZ*) gene that prevented the enzyme from being expressed, indicating a positive colony with an insertion in *lacZ*. Blue pigmented colonies appeared through the metabolism of the X-Gal, indicating that no insert disrupted *lacZ*. White colonies were screened using PCR with M13 forward and reverse primers in order to verify the presence of the insert within the pTOPO 2.1 vector. Colonies containing the desired inserts were grown overnight in a LB broth culture and then used to isolate the plasmid DNA via a QIAprep Miniprep purification kit.

Plasmid Construction

Plasmids were sequentially constructed by digesting the isolated plasmids from the minipreps with various endonucleases, depending on the recipient vector and the insert (Fig. 1). The digestion was allowed to incubate overnight at 37˚C before gel electrophoresis was used to separate the plasmid fragments in a 0.8% agarose gel. Long wavelength UV was used to visualize the banding in order to reduce DNA damage. The appropriate bands were cut out from the gel and purified using a silica (glassmilk) purification procedure. The purified digested inserts and vectors were then ligated using T4-DNA ligase and transformed into NEB 10-beta *E. coli* competent cells. Transformants were grown on LB agar plates with the antibiotics that corresponded to the resistance(s) on the vector. Colony PCR was used to screen the colonies that grew on the LB agar plates for the correct size of insert using specific primers designed in our lab (Table 1).

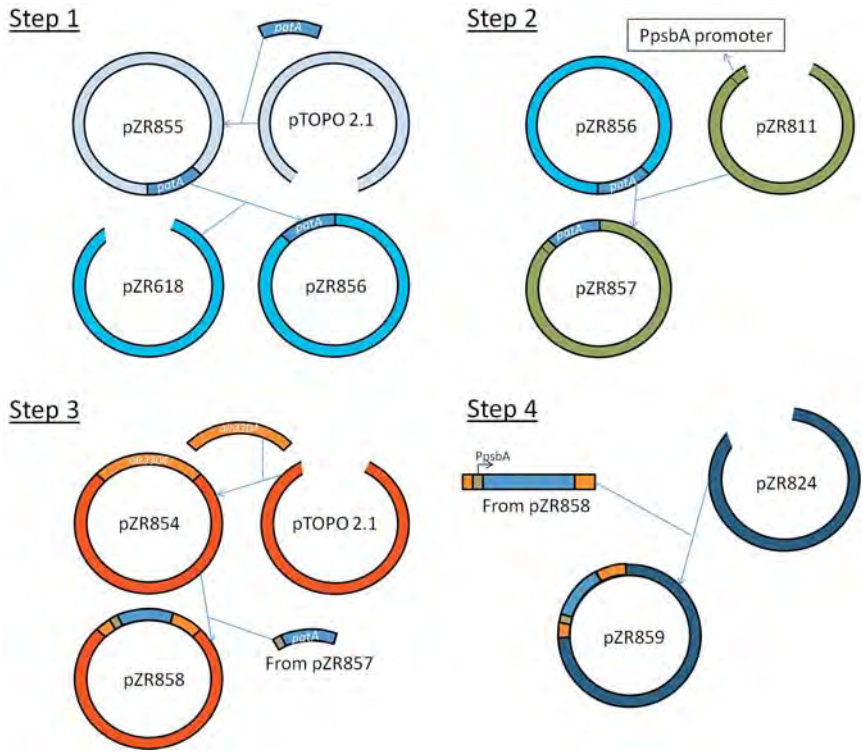

Figure 2. Plasmid construction outline. (Step 1) Amplified DNA from the *Anabaena* genome is inserted into a pTOPO 2.1 vector. Then *patA* is removed with restriction enzymes such that NdeI-*patA*-SalI is the insert. This fragment is then inserted into NdeI-SalI digested pZR618, creating pZR856, and transformed into *E. coli*. (Step 2) pZR856 is isolated and digested to provide a BamHI-*patA*-XhoI fragment which is ligated to BglII-XhoI digested pZR811, fusing the insert to the *PpsbA* promoter and creating pZR857. (Step 3) *Alr3304* amplified from the *Anabaena* genome is inserted into a pTOPO 2.1 vector, creating pZR854. NruI-*PpsbA*-*patA*-XhoI is removed from pZR856 and inserted to HpaI-SalI site within *alr3304* to create pZR858, knocking out *alr3304*. (Step 4) A BamHI-3.7kb-XhoI fragment is removed from pZR858 and inserted into BglII-XhoI digested pZR824 to create pZR859. This plasmid can then be used for conjugative transfer into *Anabaena*.

RESULTS AND DISCUSSION

In order to create the desired mutant containing an over-expression of *patA* and a knock-out of *alr3304*, the genes were isolated from the genomic DNA of *Anabaena* 7120 (Fig. 3). The amplified *patA* was 1.2kb in length and targeted using primers created by our lab, ZR193 and

ZR194. *Alr3304* was amplified using the upstream primer ZR191 and the downstream primer ZR192, yielding an amplicon of size 3.0kb. Both amplified products were the expected sizes.

The amplified products of the PCRs were cloned into pTOPO 2.1 vectors, which would be used to transfer the isolated genes into other vectors. Plasmids containing *alr3304* were named pZR854, while plasmids with *patA* were named pZR855.

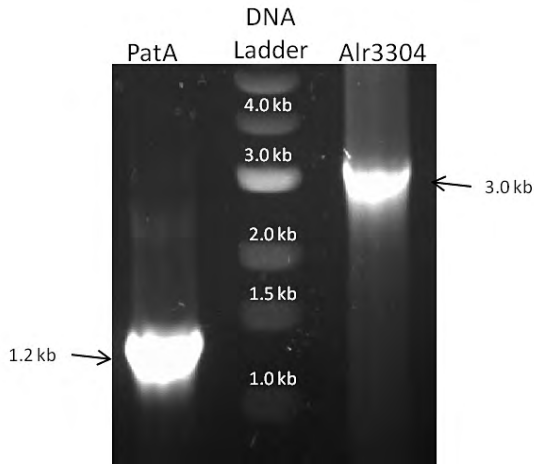

Figure 3. *PatA* and *alr3304* amplification. Primers ZR193 and ZR194 were used to amplify *patA* from *Anabaena* genomic DNA using PCR. The resulting amplicon was 1.2kb in length. *Alr3304* was amplified from *Anabaena* genomic DNA using PCR with primers ZR191 and ZR192. An amplicon of 3.0kb resulted from PCR.

Transformants were selected using the antibiotic resistance of kanamycin and amplicillin. The isolated colonies were tested with M13F and M13R primers to verify the presence of the inserts (data not shown). Also, isolated plasmid DNA pZR855 and pZR854 were sequenced to verify the sequence of the inserts within the respective plasmids. The sequencing results showed that the genes *patA* and *alr3304* were in their respective plasmids correctly (data not shown). These sequenced plasmid samples were then used to create further plasmids.

Using the restriction enzymes NdeI and SalI, *patA* was removed from pZR855, creating a segment NdeI-*patA*-SalI. The segment was transferred to the vector pZR618, cut with the same restriction enzymes, and produced pZR856. Colonies were selected using ampicillin resistance from pZR618, and PCR was used to confirm the presence of the inserts within the transformants. The usage of PCR primers T7 and T7Term (Table 1) produced an amplicon the size of 1.2kb, indicating the presence of *patA* within pZR856 (Fig. 4).

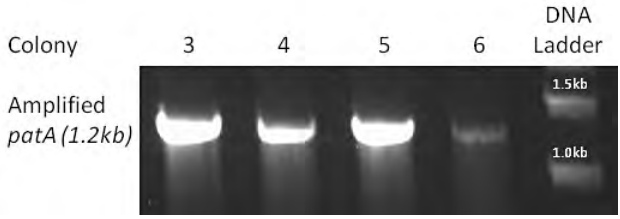

Figure 4. Colony PCR amplification of *patA* in pZR856. After *E. coli* transformation with pZR856, colony PCR was used to amplify the segment of plasmid DNA where *patA* was inserted. The primers T7 and T7 term were used to identify the correct insert. Only colonies with strong amplification were stored and used in further experiments.

Isolated plasmid DNA pZR856 was used to create pZR857 by digesting pZR856 with the restriction enzymes BamHI and XhoI, creating a segment BamHI-*patA*-XhoI, which was inserted into BglII-XhoI digested pZR811. This plasmid construction represents an important step in the execution of the whole goal of this research. By inserting *patA* into pZR811 at a specific location, the *Anabaena* promoter *PpsbA* became linked to *patA*. Attaching the promoter to *patA* will enable PatA to be produced in excessive amounts through normal cell functions, causing an increased ratio of heterocysts to vegetative cells (5). Transformed *E. coli* were selected for with kanamycin resistance from pZR811 and tested for the presence of the insert *PpsbA-patA* with PCR primers ZR127 and ZR194 (Table 1). Results of the PCR showed the correct amplified product, shown by a band with a size of roughly 1.6kb (Fig. 5). This verifies that the promoter was correctly attached to *patA*, enabling further plasmid development.

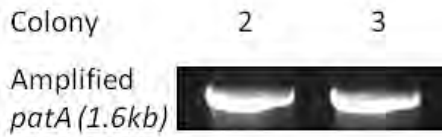

Figure 5. Colony PCR amplification of *patA* in pZR857. Primers ZR127 and ZR194 were used to amplify the region of plasmid DNA containing *patA*. This region also contains the promoter *PpsbA*, accounting for the increase in amplicon size.

With the creation of pZR857, the product *PpsbA-patA* can be inserted within *alr3304* of pZR854 to create the desired knock-out. pZR857 was digested with restriction enzymes NruI and XhoI, creating the insert NruI-*PpsbA-patA*-XhoI. The insert was ligated to HpaI-SalI digested pZR854, creating pZR858. This new plasmid contained the *alr3304* with *PpsbA-patA* inserted within it in order to create the knock-out. *E. coli* containing the correct plasmids were selected for using ampicillin and kanamycin resistance. Upon isolation of *E. coli*, pZR858 was verified with PCR using primers M13R and ZR194. The correct size of the amplified region is 2.7kb in length, which was seen with visualization of the gel under UV light (Fig. 6). Work proceeded with the construction of pZR859. However, PCR of *E. coli*

containing pZR859 showed a lack of the desired insert, length 3.7kb. Results of enzymatic digestion of pZR859 with SalI also concurred with PCR results; the enzyme digestion should have produced fragments of size 5.3kb, 2.6kb, and 1.6kb. However, only a plasmid DNA band and a band of size 6.5kb were seen (data not shown). Therefore, construction of pZR859 was unsuccessful.

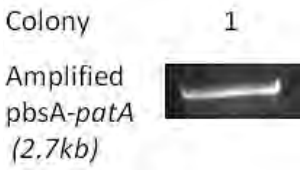

Figure 6. Colony PCR amplification of *alr3304-PpsbA-patA* in pZR858. The primers M13R and ZR194 were used to amplify the 2.7kb segment of plasmid pZR858 containing *PpsbA-patA* that was inserted into *alr3304*. The length of the amplicon is expected to be 2.7Kb.

Future directions with this research entail fixing the problems in pZR859. Once the insert has been verified within pZR859, the recombinant *E. coli* will be conjugated with *Anabaena* 7120 in order to transfer the insert into the genomic DNA of *Anabaena*. This process will be done through double cross-over. Both ends of the *PpsbA-patA* fragment have both (5'and 3') flanking sequence of *alr3304,* which will allow the entire fragment to be inserted into the genomic location of *alr3304*. Such a double cross-over recombinant will both silence *alr3304* and over-express *patA*. This recombinant *Anabaena* will theoretically produce more heterocysts than either of the two separate mutants (5, 10). An increase in heterocyst formation will then enable the cyanobacteria to produce a higher amount of ammonia than would be normal. Using a photobioreactor, the cyanobacteria can be grown in large quantities on cheap solar energy and nitrogen and carbon dioxide from the atmosphere. Also, as long as essential nutrients are being supplied, the cyanobacteria will not need replacing. This continuous production of ammonia has the possibility to change the ammonia production industry in drastic ways, both reducing costs and environmental pollution.

ACKNOWLEDGEMENTS

I thank Chuck Halfmann and Kangming Chen for the help they provided throughout the course of my research and the Joseph Nelson Mentorship program for support and funding.

REFERENCES

1. Campbell, E. L., M. L. Summers, H. Christman, M. E. Martin, and J. C. Meeks. 2007. Global Gene Expression Patterns of *Nostoc punctiforme* in Steady-State Dinitrogen-Grown Heterocyst –Containing Cultures and at Single Time Points during the Differentiation of

Akinetes and Homogonia. J. Bacteriol. 189(14): 5247-5256. Retrieved from http://www.ncbi.nlm.nih.gov/pmc/articles/PMC1951844/?tool=pmcentrez.

2. Fleming, H., and R. Haselkorn. 1973. Differentiation in *Nostoc muscorum*: Nitrogenase Is Synthesized in Heterocysts. Proc Nati Acad Sci USA. 70(10): 2727-2731. Retrieved from http://www.ncbi.nlm.nih.gov/pmc/articles/PMC427096/?tool=pmcentrez.
3. Frumkin, H., J. Hess, and S. Vindigni. 2009. Energy and Public Health: The Challenge of Peak Petroleum. Public Health Rep. 124: 5-19. Retrieved from http://www.ncbi.nlm.nih.gov/pmc/articles/PMC2602925/?tool=pmcentrez.
4. International Fertilizer Industry Association. 2009. Fertilizers, Climate Change and Enhancing Agricultural Productivity Sustainably. Paris, France: International Fertilizer Industry Assoction. Retrieved from http://www.fertilizer.org/ifa/HomePage/LIBRARY/Publication-database.html/Fertilizers-Climate-Change-and-Enhancing-Agricultural-Productivity-Sustainably.html.
5. Liang, J., L. Scappino, and R. Haselkorn. 1992. The *PatA* Gene Product, Which Contains a Region Similar to CheY of *Escherichia coli*, Controls Heterocyst Pattern Formation in the Cyanobacterium *Anabaena* 7120. Proc Nati Acad Sci USA. 89: 5655-5659.
6. Meeks, J. C., E. L. Campbell, M. L. Summers, and F. C. Wong. 2002. Cellular Differentiation in the Cyanobacterium *Nostoc punctiforme*. Arch Microbiol. 178: 395-403.
7. Orozco, C. C., D. D. Risser, and S. M. Callahan. 2006. Epistasis Analysis of Four Genes from *Anabaena* sp. Strain PCC 7120 Suggests a Connection between *PatA* and *PatS* in Heterocyst Pat-ter Formation. J. Bacteriol. 188(5): 1808-1816. Retrieved from http://www.ncbi.nlm.nih.gov/pmc/articles/PMC1426565/?tool=pmcentrez.
8. Risser, D. D., and S. M. Callahan. 2008. HetF and PatA Control Levels of HetR in *Anabaena* sp. Strain PCC 7120. J. Bacteriol. 190(23): 7645-7654. Retrieved from http://www.ncbi.nlm.nih.gov/pmc/articles/PMC2583621/?tool=pmcentrez.
9. Schrock, R. R. 2006. Reduction of Dinitrogen. PNAS. 103(46): 17087. Retrieved from http://www.ncbi.nlm.nih.gov/pmc/articles/PMC1859893/?tool=pmcentrez.
10. Wolk, C. P., A. Conklin, Z. Kong, S. Lechno-Yossef, J. Liu, and E. Wojciuch. 2009. Developmental Biology of Nitrogen-Fixing Cyanobacteria. MSU-DOE Plant Research Laboratory Forty-Fourth Annual Report 2009. 100-106.
11. Woods, J., A. Williams, J. K. Hughes, M. Black, and R. Murphy. 2010. Review: Energy and the food system. Phil. Trans. R. Soc. 365: 2991-3006. Retrieved from http://www.ncbi.nlm.nih.gov/pmc/articles/PMC2935130/?tool=pmcentrez.